Supporting Information

Construction of Amorphous/Crystalline Fe doped CoSe for Effective Electrocatalytic Oxygen Evolution

Wenjuan Chen, ‡ Qian Zhang, ‡ Youzheng Zhang, Caidi Han, Jinting Wu, Jian Gao, Xiao-Dong Zhu,*

Yong-Chao Zhang*

State Key Laboratory Base of Eco-Chemical Engineering College of Chemical Engineering, Qingdao

University of Science & Technology, Qingdao, China

*Corresponding authors. E-mail addresses: yongchaozhang@qust.edu.cn (Y.-C. Zhang), xiao-

dong_zhu@qust.edu.cn (X.-D. Zhu).

1. Experimental methods

1.1 Synthesis of catalysts

The nickel foam was cut into integrated "convex" shaped pieces of 1×1 cm^2, and washed with 3.0 M HCl for 10 min to remove the oxide layer on the nickel foam surface. Surface oils were removed by ultrasonic washing with acetone for 10 min, followed by sequential ultrasonic washing with ethanol and ultrapure water for 10 min, and drying in a vacuum oven overnight for further use. Working electrode was prepared by cyclic voltametric electrodeposition using a three-electrode system in the corresponding solution with a voltage range of -0.3 V to -0.8 V (*vs.* Ag/AgCl), where the number of electrodeposition revolutions was 2 and the electrodeposition time was 200 s.

The preparation method of Fe-doped CoSe electrodeposition solution is as follows: first, Co(NO$_3$)$_2$·6H$_2$O (40 mM), SeO$_2$ (35 mM) and LiCl (200 mM) were added to 100 mL of water and ultrasonicated to dissolve them completely. After the mixed solution was passed through Ar$_2$ for 20 min to remove the air, FeSO$_4$·7H$_2$O (10 mM) was quickly added to the above solution. Oxygen was removed by passing Ar$_2$ gas for 10 min, and the electrodeposition solution was deoxygenated to inhibit the oxidation of divalent iron to trivalent iron. Fe-CoSe/NF-1, Fe-CoSe/NF, Fe-CoSe/NF-2, Fe-CoSe/NF-3, Fe-CoSe/NF-4 electrodes were synthesized in Fe^{2+}/Co^{2+} solution (molar ratio 1: 5, 1: 4, 1: 3, 1: 2, 1: 1), and the total amount of metal ions (Fe^{2+}and Co^{2+}) was maintained at 50 mM. In addition, CoSe/NF and FeSe/NF electrodes were prepared in solutions without Fe^{2+}and Co^{2+}.

The preparation method of Co-doped FeSe electrodeposition solution is as follows: SeO$_2$ (35 mM) and LiCl (200 mM) were added to 100 mL of water and ultrasonicated to dissolve them completely. After the mixed solution was passed through Ar$_2$ for 20 min to remove the air, FeSO$_4$·7H$_2$O (a mM) was quickly added to the above solution. Oxygen was removed by passing Ar$_2$

gas for 10 min, and the electrodeposition solution was deoxygenated to inhibit the oxidation of divalent iron to trivalent iron. Then add $Co(NO_3)_2 \cdot 6H_2O$ (b mM) and pass Ar_2 10 min. Where a and b correspond to 40 mM and 10 mM and 33.33 mM and 16.67 mM, respectively.

1.2 Characterization methods

High-resolution transmission electron microscopy (HR-TEM) analysis was performed under a Tecnai G2F20 transmission electron microscope with an accelerating voltage of 200 kV. X-ray diffraction (XRD) analysis was carried out on a D/MAX-2500 Kα-ray diffractometer equipped with 0.154 nm Cu Kα radiation at a scan rate of 5°/min. X-ray photoelectron spectroscopy (XPS) analysis was performed on a PHI5000 using Al Kα radiation, and the C 1s peak (284.8 eV) of contaminated carbon was used to calibrate the binding energy.

1.3 Electrochemical testing

OER performance measurements were performed at room temperature on a CHI760E electrochemical workstation with 1 M KOH electrolyte using a three-electrode system. Potassium hydroxide was purchased from Aladdin with a purity of 99.99% (electronic grade), and the electrolyte was free of Fe^{3+} ions (<1 ppm) after dilution with 18.2 MΩ·cm ultrapure water. The reference electrode was a Ag/AgCl electrode, and the counter electrode was a graphite rod electrode.

Linear sweep voltametric curves (LSV) were tested over a voltage range of +1.1 V to +1.7 V (vs. RHE) at a scan rate of 5 mV/s, and the results were corrected with iR. Cyclic voltammetry (CV) was performed at a scan rate of 100 mV/s until the electrode reached a steady state. Then linear scanning voltammetry (LSV) was performed at a scan rate of 2 mV/s. The time current curve (i-t) was tested at a voltage of 1.51V (vs. RHE). Electrochemical impedance spectroscopy (EIS) was

performed in the frequency range of 100 kHz to 0.1 Hz. The electrochemical active surface area (ECSA) of the catalyst was calculated by the formula of $ECSA=C_{dl}/C_s$ and $Cs=40 \mu F/cm^2$. The turnover frequency (TOF) value was calculated by the formula $TOF=1*I/(4*n*F)$ in 1 M phosphate buffer solution (pH=7.00), where I is the current obtained from the polarization curve. $n=Q/F=(It)/F=(I*V/\mu)/F=(S/\mu)/F$, where S is the effective area calculated from the CV cycle and μ is the scan rate of 50 mV/s. The measured voltage was converted to the reversible hydrogen electrode voltage using the Nernst equation ($E_{RHE} = E_M + 0.059 \times pH + 0.109$, where E_{RHE} is the reversible hydrogen electrode voltage, where E_M is the measured voltage).

1.4 OER performance testing

We performed XPS characterization of Fe-CoSe/NF samples after stability testing. As shown in **Fig. S8-10**, after the stability test, the Fe 2p orbital in Fe-Cose /NF shifts towards the direction of high binding energy, and the content of Fe^{3+} increases, which accelerates the OER reaction process.[1] For the Co 2p orbital, the binding energy of Co $2p_{3/2}$ shows a positive shift of 0.5 eV to a higher binding energy, indicating that Co can partially form a higher valence state after stability testing.[2] For the Se3d orbital, the peaks of Se $3d_{5/2}$ and Se $3d_{3/2}$ are largely gone, and the proportion of selenium oxides is larger. These phenomena indicate that an oxidation reaction occurs during the OER process, and Se is oxidized to form SeO_x.
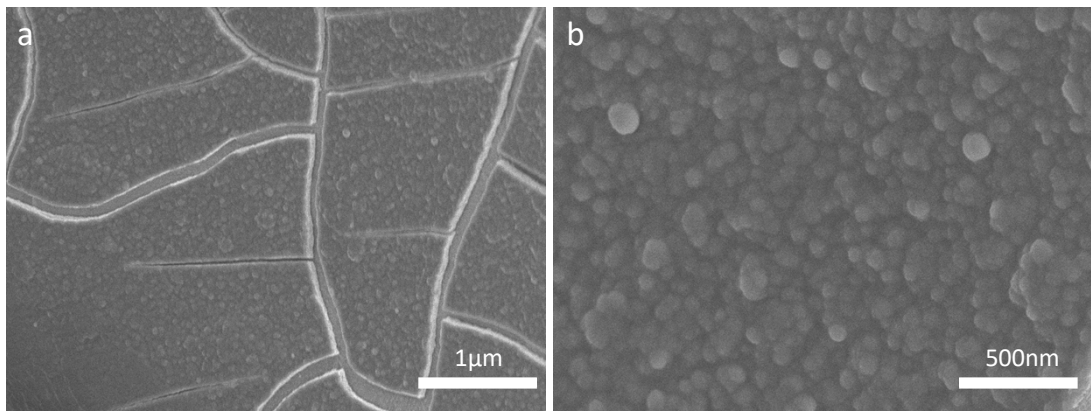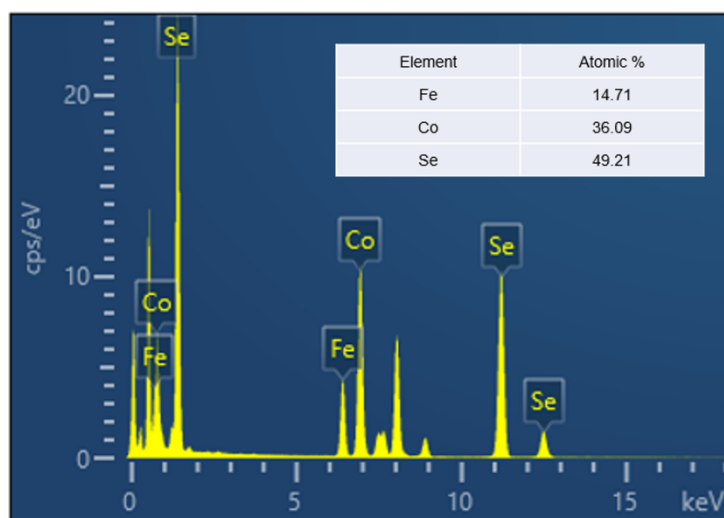
Fig. S1 SEM images of Fe-CoSe/NF

Element	Atomic %
Fe	14.71
Co	36.09
Se	49.21

Fig. S2 EDS characterization with element content of Fe-CoSe.
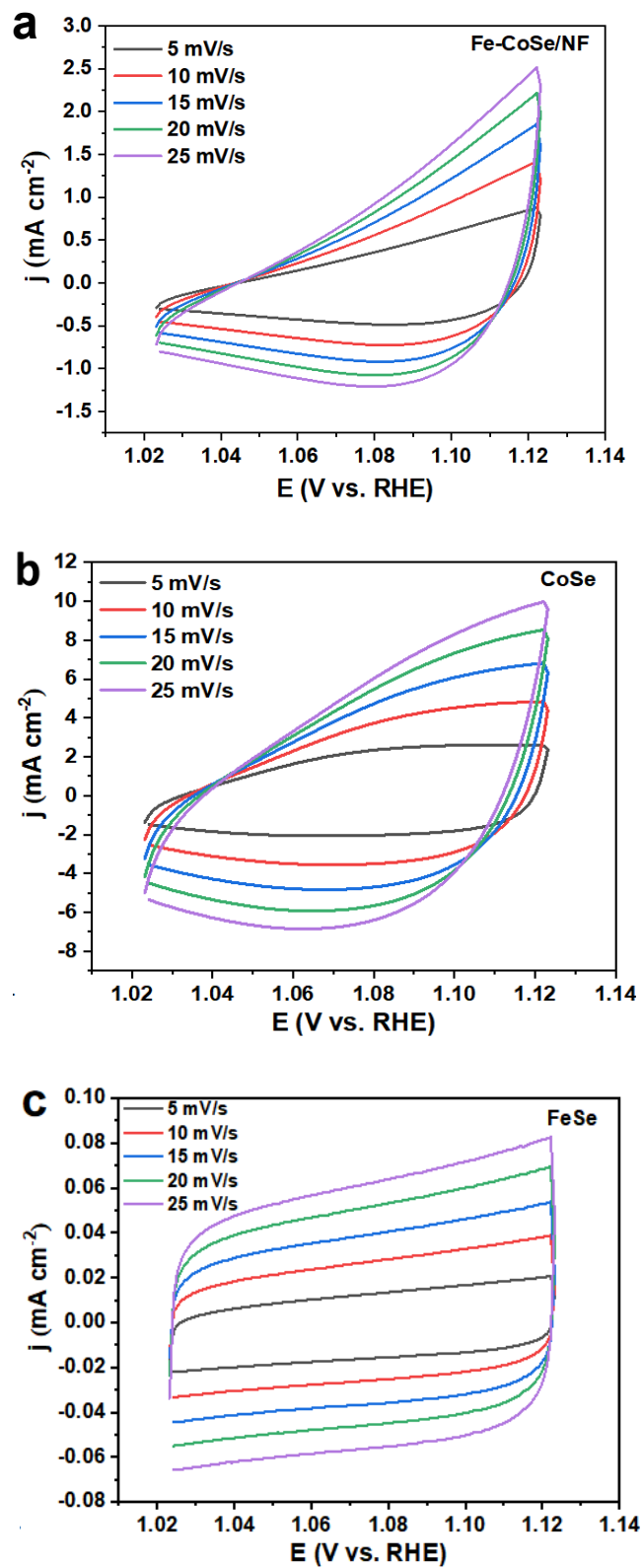
Fig. S3 The CV of Fe-CoSe/NF **(a)**, CoSe/NF **(b)**, and FeSe/NF **(c)** at different scanning speeds.
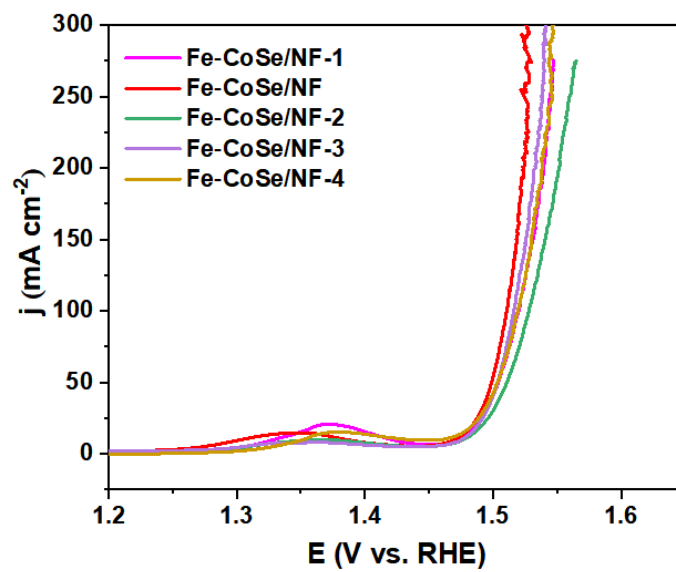
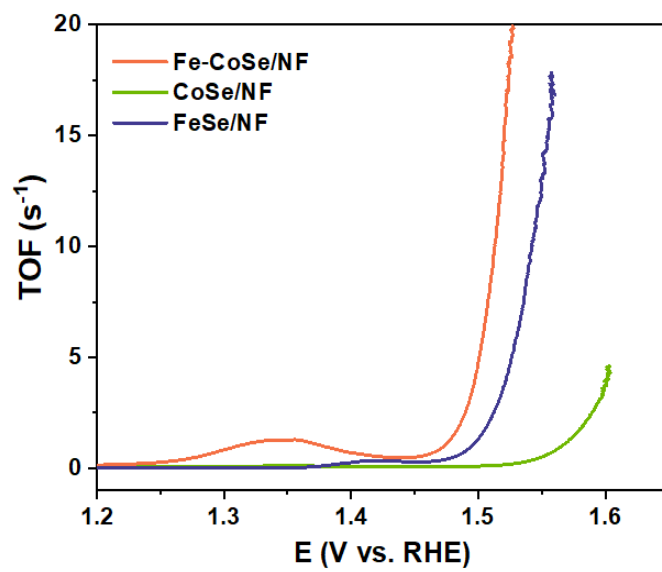**Fig. S4** The LSV of Fe-CoSe/NF-1, Fe-CoSe/NF, Fe-CoSe/NF-2, Fe-CoSe/NF-3 and Fe-CoSe/NF-4 samples.

Fig. S5 TOF values of samples.
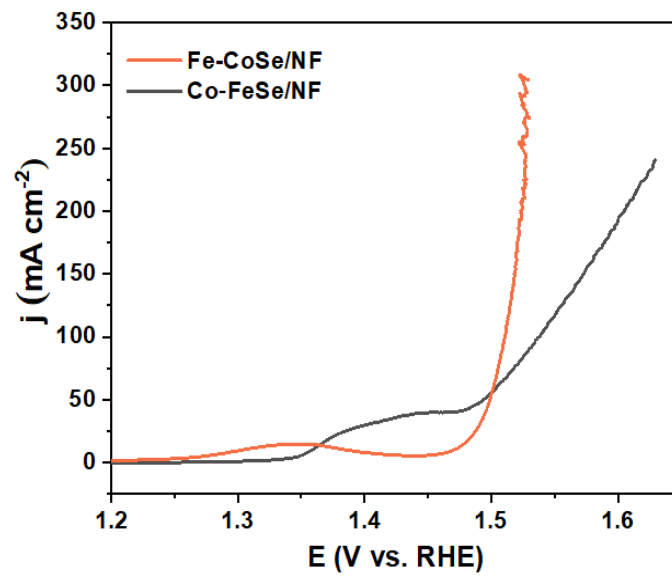
Fig. S6 The LSV of Fe-CoSe/NF, Co-FeSe/NF.
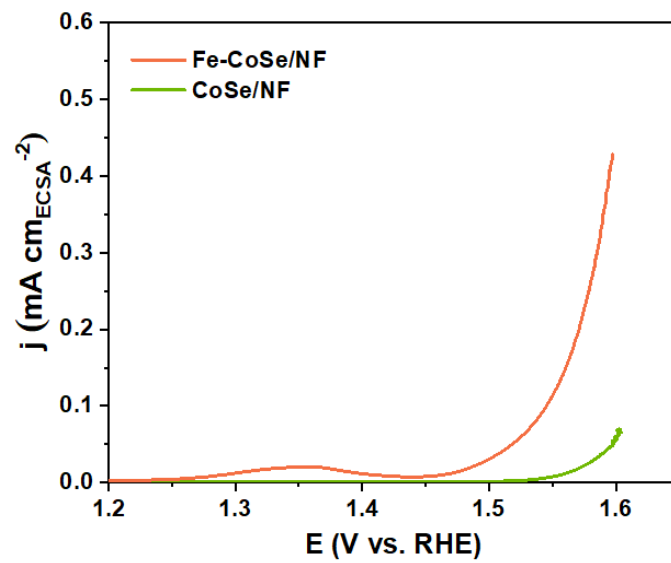
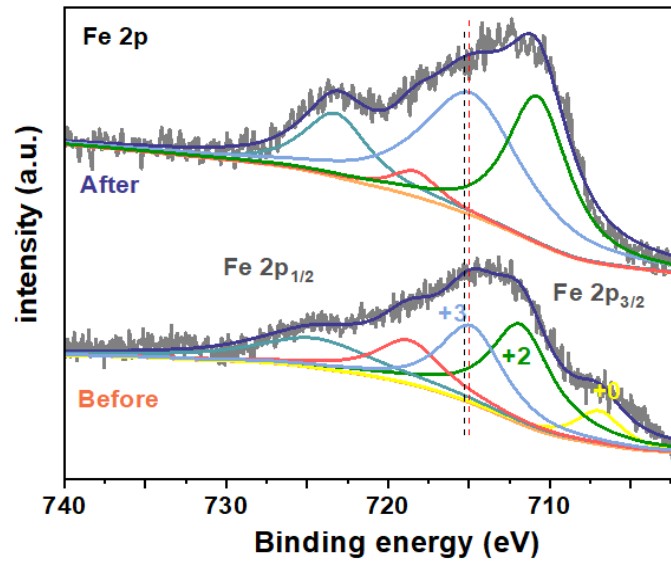**Fig. S7** The LSV curve after electrochemical surface area (ECSA) normalized calculation.
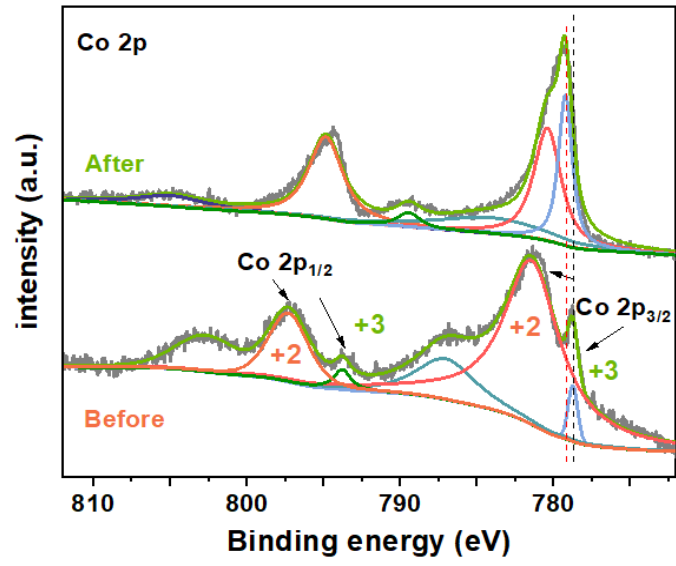
Fig. S8 XPS spectra of Fe 2p of samples.
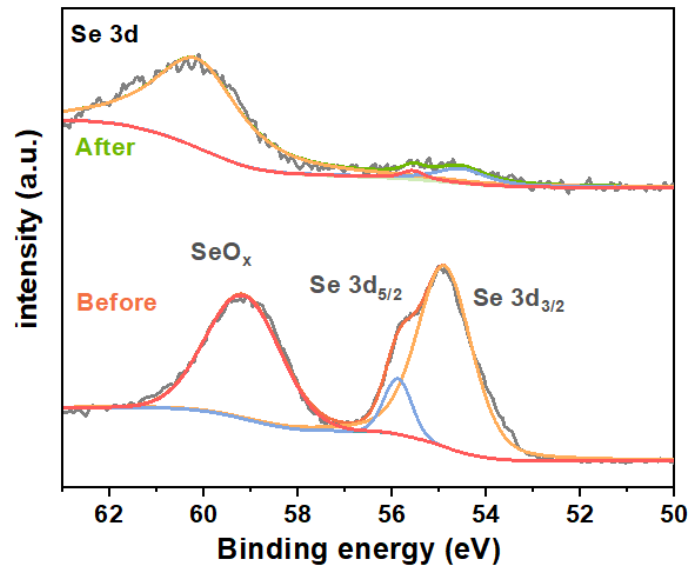
Fig. S9 XPS spectra of Co 2p of samples.

Fig. S10 XPS spectra of Se 3d of samples

Table S1. OER catalyst performance comparison with other samples.

Catalyst	j/ mA/cm^{-2}	η/V at the corresponding J	Substrate	Electrolyte	References
Fe-CoSe/NF	**50** **100**	**269** **280**	**Ni foam**	**1 M KOH**	**This work**
NiFeO$_x$H$_y$/ NF-x	50 100	276 306	Ni foam	1 M KOH	*Chemical Engineering Journal* **2024**, 482, 148887
Ag/NCMO/ NF	50 100	277 299	Ni foam	1 M KOH	*Advanced Functional Materials* **2022**, 32(7), 2107056
Co$_2$P-Ni$_3$S$_2$/NF	50 100	313 332	Ni foam	1 M KOH	*Small* **2023**, 19(50), 2304081
FeS$_2$ MS/NF	50 100	283 314	Ni foam	1 M KOH	*Applied Catalysis B: Environmental* **2023**, 339, 123171
Ni$_3$S$_2$/NiO	50 100	310 320	Ni foam	1 M KOH	*Chemical Engineering Journal* **2023**, 475, 146140

Reference

[1] Z. C. Gong, R. Liu, H. S. Gong, G. L. Ye, J. J. Liu, J. C. Dong, J. G. Liao, M. M. Yan, J. B. Liu, K. Huang, L. L. Xing, J. F. Liang, Y. M. He and H. L. Fei, *ACS Catal.*, 2021, **11**, 12284-12292.

[2] J. Y. Zhang, Y. Yan, B. B. Mei, R. J. Qi, T. He, Z. T. Wang, W. S. Fang, S. H. Zaman, Y. Q. Su, S. J. Ding and B. Y. Xia, *Energy Environ. Sci.*, 2021, **14**, 365-373.

[3] J. Deng, Z. C. Wang, H. Yang, R. Jian, Y. F. Zhang, P. Xia, W. Liu, O. Fontaine, Y. C. Zhu, L. M. Li and S. Chen, *Chem. Eng. J.*, 2024, **482**, 148887.

[4] D. Li, Y. Y. Qin, J. Liu, H. Y. Zhao, Z. J. Sun, G. B. Chen, D. Y. Wu, Y. Q. Su, S. J. Ding and C. H. Xiao, *Adv. Funct. Mater.*, 2022, **32**, 2107056.

[5] H. X. Li, X. L. Gao and G. Li, *Small*, 2023, **19**, 2304081.

[6] C. Z. Yue, X. N. Zhang, J. Yin, H. W. Zhou, K. Liu and X. Liu, *Appl. Catal. B-Environ.*, 2023, **339**, 123171.

[7] F. T. Luo, W. T. Liu, Y. Liu, P. Yu, X. Jiang and S.J. Chen, *Chem. Eng. J.*, 2023, **475**, 146140.